CHALMERS

Improving adhesion between Carbon Fibre Reinforcements and Alkali-Activated Cements.

Masters Thesis

Derk de Muinck

The Department of Chemistry and Chemical Engineering
CHALMERS TEKNISKA HÖGSKOLA
Gothenburg, Sweden 2020

Abstract

Concrete is the most widely used material in the world and even though as a material it has a relatively low environmental impact the shear amount of it being used is cause for environmental concerns. Reducing the need for large quantities of concrete and finding alternatives materials are two ways to reduce its impact. This can be achieved by using carbon fibre reinforcements instead of steel rebars as well as using slag cement instead of conventional Portland cement. This project seeks to improve the adhesion of carbon fibre reinforcements to the slag cement by impregnating the fibre bundles with a solgel. The fibre bundles were individually impregnated in different solgel baths and embedded into slag cement pucks. The shear strength was subsequently measured through pullout testing and the degree of impregnation was examined under a microscope. A wide range of different solgels were tested and the purely inorganic solgels showed higher shear strengths than the textile reinforcements used in the industry today. The microscopy showed a thorough impregnation although it was difficult to quantify. While these results were promising there was a large amount of variance in the results due to the simplicity of the methods used. Future work should focus on refining these methods and continue to expand upon the potential of the coatings studied in this project.

Abbreviations

- TRC - Textile reinforced cement
- OPC - Ordinary portland cement
- TEOS - Tetraethyl orthosilicate
- Ormosil - Organically modified silicate
- GLYMO - (3-Glycidyloxypropyl)trimethoxysilane
- VTMOS - Vinyltrimethoxysilane
- MEMO - 3-(trimethoxysilyl)propyl methacrylate
- PTMOS - Trimethoxy(propyl)silane
- PAN - Polyacrylonitrile
- Calc. - Calculated
- Pot. - Potential
- ISS - Interfacial shear strength

Contents

1 Introduction

There is no other material in the world that is more widely used than concrete and demand is growing[1]. By 2050 the world is expected to use four times as much concrete than it did in 1990 and in 2017 over 4 billion metric tons were produced [2]. Because of the scale of concrete production it is of course also a cause of a large carbon footprint. Cement which together with gravel is a main component of concrete stands for 7% of the world's CO_2 emissions, more than all of the world's trucks combined [3]. Therefore finding alternative methods of producing cement is a key element of reducing the CO_2 emissions.

Finding an alternative way to reinforce concrete is another key aspect of reducing cement's carbon footprint. Conventionally concrete is reinforced with steel rebars to increase its durability, however steel is prone to corrosion [4]. If a non-corroding material were used instead, such as carbon fibre bundles, it would be possible to produce thinner and lighter structures [5]. Thus concrete usage and thereby demand could be reduced.

These two solutions are the focus of this thesis. Reinforcing slag cement, which is a byproduct from iron manufacturing, with carbon fibres bundles. By attempting to increase adhesion between carbon fibre bundles and slag cement this thesis aims to expand the areas where those solutions are viable.

1.1 Background

This thesis is part of a larger project called "Green cement based on blast furnace slag" which is a collaboration between academic and industrial partners. It is divided into three different work packages. The first is mainly done at Chalmers University of Technology and focuses on the properties and structure of ground granulated blast furnace slag and fly ash cement in relation to synthesis and processing. In other words the development of an alternative to conventional cement.

The second work package which includes this thesis work focuses on evaluating commercial reinforcement structures and to develop novel reinforcements with improved adhesion to slag based cement. It also aims to manufacture and evaluate specimens and conceptual demonstrators. This work is mainly performed at RISE SICOMP.

The third work package is in collaboration with a multitude of industrial partners and has the objective to identify the potential advantages and drawbacks to implementing and developeing materials on an industrial scale. The industrial partners are SSAB Merox, Gunnebo, Stena Recycling International, S:t Eriks, and GKN.

Previous work on the second package faced problems due to incomplete fibre impregnation [6]. Therefore this project focuses on the use of solgels which have a particle size in the nanoscale range and should be able to impregnate more thoroughly.

1.2 Aim

The aim of this project is to examine the potential of different solgel coatings to improve the shear strength between slag cement and a carbon fibre bundle.

2 Theory

This chapter describes the theory used to develop the methods for this project. At first a general description of textiles reinforcements is given and then the chemical theory for both the coating and

the cement is described. Finally the physical challenges that need to be overcome to maintain the solgel coating and coat the fibre bundles thoroughly.

2.1 Textile reinforced concrete

Concrete is a composite material where gravel particles are bound together by a cement matrix which is often reinforced with steel rebars [4]. Textile reinforcements are natural or synthetic fibre bundles woven into a mat. That mesh is then subsequently incorporated into a cement to reinforce it as shown in figure 1 to replace the need for steel rebars [7]. The end goal of this incorporation is to strengthen the cement to strain. Commercially this reinforcement is usually performed with steel rebars. Steel however has low flexural strength and is prone to corrosion. Normally steel is protected from corrosion by an extra layer of cement but this is not necessary with carbon fibres. Typical cross sections for conventional concrete is 100-300mm while TRC's usually are less than 50 mm across [5]. This results in TRC being less material intensive than its conventional counterpart.

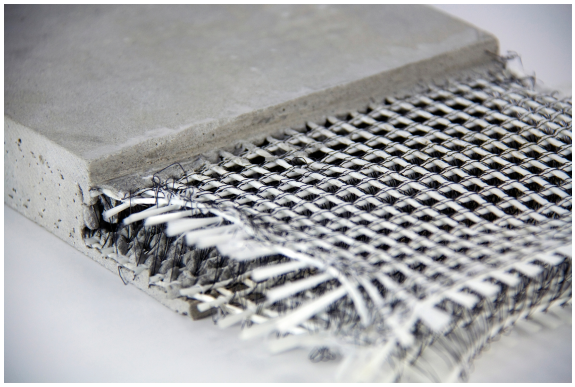

Figure 1: Fibre reinforcements integrated into concrete[8].

The fibres that are typically used in the industry today are impregnated with epoxy or styrene-butadiene. There have been attempts made in the industry to replace this impregnation with a different material to improve adhesion to the matrix [9]. By increasing the fibre adhesion one improves upon the overall composite. If a fibre slips because adhesion is sub par it is regarded as a defect in the material [10]. Therefore the main focus of this thesis was to find a suitable replacement to this impregnation using the solgel method.

2.2 Solgel

The definition of solgel is hinted at by its name. It is partly a colloidal suspension or solution/sol and also a polymer network or gel. In order to make a sol gel one must undergo a process consisting of three distinct steps complex formation, hydrolysis, and polycondensation [11]. The need for complex formation depends on what sol gel one is attempting to make, often it is possible to buy a previously formed complex. The latter two steps using a silica alkoxide complex are shown in figure 2 [12].

The end result of hydrolysis is replacing one of the OR groups with an hydroxide group. The step also produces an alcohol. The condensation step can take place in two different ways, either through water condensation or through alcohol condensation and both usually occur simultaneously. Both forms of condensation propagate a polymerization of the silica alkoxide but produce different side products, water and alcohol. Both are usually present at the start of the reaction. Water is

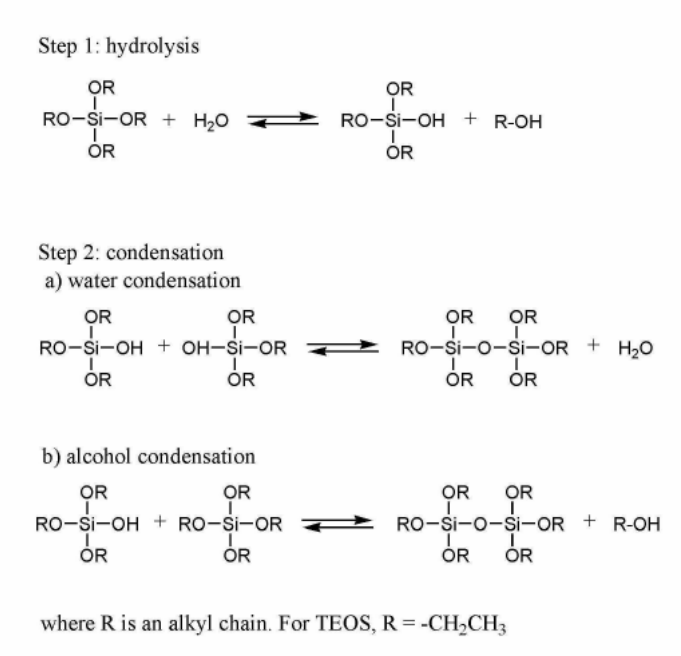

Figure 2: The different steps taken to form a sol gel.

required for hydrolysis and alcohol is in most cases added as a solvent. Therefore neither of these side products need to be removed from the subsequent gel [13].

The polymers link cyclically with themselves forming discrete particles which link together building a chain network [13]. Thus a a network of particles in solution receives gel like properties.

The size and nature of the different particles in a sol gel is determined in part by pH, type of complex, and H_2O:Si ratio. It is the relative reaction rates of the condensation reaction to the hydrolysis reaction which determines the size of the particles [14] and all of those factor play a role in controlling those rates.

The hydrolysis reaction can be catalyzed with both acids and bases but result in different kinds of sol gels. When catalyzed with a base silica tends to bundle up into particles and a more colloidal solution is made, chains of these colloids then proceed to polymerize. Acid catalyzed reactions polymerize more before becoming colloids and branch out throughout the solution making one network. The differences can be observed in figure 3.

In figure 3 the acid catalyzed network forms because the hydrolysis reaction is much faster than the condensation reaction and vice versa for the base catalyzed sol gel. For some silica alkoxides such as TEOS the acidic catalyzation behaves differently below a pH of 2 because at this point it reaches SiO_2's isoelectric point. The surface charge becomes zero and therefore very little reaction can take place. Below the isoelectric point however very limited branching and a microporous structure is formed out of small particles with a diameter under 2nm [15].

The ratio of Si, EtOH and H_2O determines if the hydrolysis and condensation reactions can be performed to completion. Theoretically a 2/1 ratio of Si and H_2O is sufficient however the formation of intermediates make that unlikely. Si precursors such as TEOS are also immiscible in water and therefore EtOH is often added as a solvent. EtOH shifts the equilibrium of the alcohol condensation however seeing as it is formed when TEOS is used as precursor. Changing these ratios can have

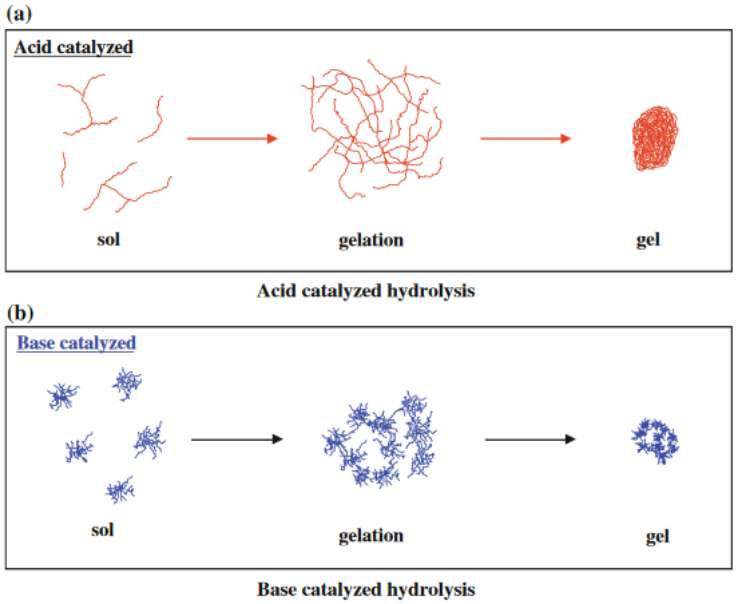

Figure 3: Formation of a gel from an acid (a) or basic (b) catalyzed hydrolysis, the change of inorganic structure from a sol to a gel

effect on the speed of the different steps of the reaction.

The complex that is formed can be changed by using different precursors. It is even possible to make a hybrid organic-inorganic networks by introducing an organic precursor. Thus a new type of organically modified silicate (Ormosil) polymer is formed.

2.3 Alkali Activated Slag Cement

Slag is a byproduct from iron manufacturing and a possible replacement for a portion of the construction industry's demand for portland cement. Ordinary portland cement's (OPC) most pollution intensive step is the burning of limestone which is avoided when producing slag cement [3]. From a life cycle perspective slag cement produces on average 73% less green house gases, requires 43% less energy and 25% less water [16]. Concretes made with slag cement have also been shown to have high strength and durability [17]. The difficulties that slag cement faces to become more widely adopted are the complex nature of the cement and a lack of wide spread availability [18]. However, its outstanding environmental profile and interesting mechanical and acid resistance make the material interesting for special applications, such as pipes, agriculture, and filtration amongst others [19].

The complex chemical composition of slag cement and OPC is seen in figure 4 [17]. While OPC's chemistry is not less complicated because it is the industry standard it has been more widely studied. There is a wide range of different oxides all of which affect the structure and make up of the cement. Many of the same oxides can be found in both OPC and slag cement but in different proportions. The most obvious differences are slag cement having almost double the amount of SiO_2 while OPC has more CaO.

Because OPC is the industry standard it has been subject to a larger range of studies. In depth rheological studies have shown how additves, superplasticizers, composition and particle size

Material	Component (oxide; wt%)										
	SiO_2	Al_2O_3	Fe_2O_3	MnO	MgO	CaO	Na_2O	K_2O	TiO_2	P_2O_5	[a]LoI
Slag	38.71	10.46	0.33	0.21	7.58	40.62	0.54	0.35	0.37	0.05	–0.30
OPC	19.32	7.90	2.69	0.06	0.81	61.81	0.11	1.02	0.23	0.06	2.90

a LoI = Loss on ignition at 1000 °C.

Figure 4: Chemical composition of blast furnace slag and 52.5R OPC (XRF analysis)[17]

distribution can be used to change OPC for a specific purpose. As of 2018 little to no such studies have been performed for slag cement [17]. One major difficulty that slag cement has to overcome is the large amount of shrinkage that occurs upon drying which leads to cracking [20]. It has however been shown that the addition of sand can reduce shrinkage as is commonly done with OPC [21].

It should be noted that before slag can be used as cement it needs to be activated with an alkaline solution such as water glass. This product is different to the normal hydration that OPC undergoes with water but has a very similar result. As can be seen in figure 4 slag has both network forming anions such as SiO_4^{2-} and AlO_4^{5-} and network modifying cations such as Ca^{2+} and Al^{3+}. When water glass is added a Ca-Al-Si-H gel is formed through polycondensation after slag deconstruction. For comparison in OPC mainly a Ca-Si-H gel is formed during hydration. The structure of this gel can differ greatly depending upon amount of activator used, slag structure and composition and the curing conditions in which the material hardens. A range of byproducts can also be found after the activation [22]. A comparison between the different products and by products of OPC hydration and slag activation can be seen in figure 5

The availability issue is mainly due to the fact that slag is a byproduct and not the focus of iron manufacturing. From a sustainability point of view it is advantageous but it does make it difficult to mass produce. Some countries will be able to produce more blast furnace slag than other simply because of the infrastructure of their industry [3]. In fact compared to total cement production the amount of slag cement has decreased from 17% in 1980 to 8% in 2014 [18]. It should be noted however that the overall production of cement has gone up in that time period. The largest cement producer in the world, China, produces around 2.4 billion tons of cement every year [23] while only around 60 million tons are made using slag [24]. In other words slag cement will never be able to replace OPC entirely but it even a partial substitution of OPC can have a significant environmental impact and therefore should still be developed.

Binder type		OPC	Alkaline cement
			$(Na,K)_2O$-CaO-Al_2O_3-SiO_2-H_2O
Reaction product	Primary	C-S-H	C-A-S-H
	Secondary	$Ca(OH)_2$	Hydrotalcite
		AF_m	$[Mg_6Al_2CO_3(OH)_{16}{\cdot}4H_2O]$
		AF_t	C_4AH_{13} $CASH_8$
			C_4AcH_{11} $C_8Ac_2H_{24}$

C = CaO, S = SiO_2, A = Al_2O_3, N = Na_2O, H = H_2O, c = CO_2

Figure 5: The products and byproducts of OPC hydration and Slag activation [22]

2.4 Bonding Theory

The coating that was developed for this thesis work aims to increase adhesion between carbon fibre and slag cement. To achieve this the bonding or integration between the carbon fibre and coating as well as the bonding or integration between the coating and the cement matrix are important. In this section each will be separately examined starting with the cement - coating system.

As described in section 2.3 slag cement forms a gel made up of silica, calcium and aluminum after activation. The gel formation process is analogous to the solgel process[25] and in theory could produce a similar structure. Silica is often added to cement to enhance different properties such as silica fume or silica nanoparticles to increase $Ca(OH)_2$ hydration[26] in order to increase the strength or reduce the curing time of cement. The nanoparticles are often produced via a solgel method [27].

During the course of the thesis three main types of solgels were studied, all of them silica based. A pure TEOS solgel, a TEOS Ormosil modified with GLYMO, and a TEOS Ormosil modified with VTMOS. Each precursor builds a different silica alkoxide polymer network that is in the nano scale when acidically synthesized [15]. It was theorized for this thesis that the solgels would be able to incorporate into the cement matrix in a similar fashion to silica nanoparticles even when used as a coating.

While the cement and the solgel coatings are chemically similar PAN based carbon fibres and solgels differ more greatly. As shown in figure 2 the solgel polymer is mainly an Si-O-Si chain while the structure of carbon fibre is a series of aromatic carbon rings linked together. Carbon fibres are mostly chemically inert however they can become functionalized through oxidation. Any bonding that occurs between silica alkoxide and the fibre is strongest with the help of functional groups such as carbonyl, oxide, hydroxyl, and even carboxyl. However the amount of functional groups that are normally present in the fibre is insufficient for adequate bonding. This can be remedied with the help of surface treatments such as plasma treatment or heat treatment [28]. As stated earlier in section 2.1 industrial textile reinforcements are often impregnated with epoxy or styrene butadiene but these are also polymers with little chemical interaction with cement.

The working theory that was assumed during this project was that purely inorganic solgels could achieve reasonable bonding through thorough impregnation despite the chemical difficulties. However if the fibre bundle is sized and the coating is an Ormosil the chemical bonding could be improved. The Ormosil coatings covalently bond organic monomers to the inorganic polymer network

[29]. Coupling agents are often present in sizings to increase chemical bonding to a composite matrix such as epoxy [10]. GLYMO and VTMOS introduce an epoxy or a vinyl group respectively because of their structure which can be seen in figure 6.

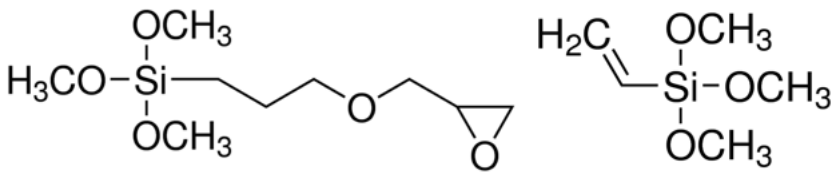

Figure 6: Structures of (3-Glycidyloxypropyl)trimethoxysilane (GLYMO)(left) and Vinyltrimethoxysilane (VTMOS)(right)

GLYMO's structure includes an epoxy group which makes it likely to bond with the coupling agents in a sizing. Moreover it has been shown that GLYMO can act as a binder and increase adhesion to polymer surfaces [30]. Carbon fibre is chemically similar to many basic polymers. VTMOS gives an Ormosil hydrophobic characteristics because of the vinyl group [31]. The fibre surface is hydrophobic both with and without a sizing which could increase bonding.

2.5 Solgel degradation

Any possible coating for a fibre cement system needs to be robust. One of the main sustainability benefits of TRC's is the longer lifetime. A coating which does not increase the bonding strength of the fibre bundle for the entirety of its lifetime is less useful. Testing the lifetime durability of the coating is beyond the scope of this project but immediate degradation was considered. Degradation can occur either chemically through hydrolysis and dissolution or physically.

Section 2.3 describes how SiO_2 reacts in an alkaline enviroment. It is assumed that the silica coating will be partly dissolved and incorparated into the cement network in a similar fashion during hardening. However, due to the limited mobility of large ions and oligomers after hardening, it is unlikely that further degradation will happen after hardening for a silica coating. The formed network will rather assume an equilibrium where some dissolution may still happen locally at the reinforcement/cement interface, but the dissolved oligomers cannot be transported away from the interface, but will rather condense again.

Hydrolysis occurs when solgel comes into contact with water according to reaction 1 [32].

$$SiO_2(s) + 2\,H_2O \longrightarrow (SiOH)_4(aq) \tag{1}$$

The kinetics of reaction 1 are slow at low pH but increases in the alkaline region [33]. To limit the reaction in an alkaline environment contact between the coating and water should be minimal. When a silica coating is used on a carbon fibre bundle the entire bundle should not be in contact with water. Water can travel via capillary forces through the fibre bundle and degrade the coating [34]. This is especially important when curing alkali activated cement in a water bath as it could contain alkaline ions.

The extent of physical degradation and hydrolysis that can take place is dependent on the composition of the solgel and the amount of TEOS. A pure inorganic TEOS coating is usually stiff and brittle. However if it is modified with an organic substrate it can become more flexible and

thicker [30]. This will result in an organically modified silicate or Ormosil. Adding organics to the silicate network also decreases the amount of Si−O−Si bonds which limits reaction 1. In studies where different amounts of organics were added to a TEOS sol-gel it was found that with increasing amounts of organics the degradation due to hydrolysis decreased [32][35]. In other words by finding the correct Ormosil one could significantly increase the robustness and handling stability of the coating.

2.6 Fibre Spreading and Impregnation

In a related project at SICOMP a fibre spreading technique was developed in order to allow efficient impregnation of carbon fibre bundles in a continuous process. The technique opened up the possibility to impregnate fibre bundles with micrometer sized particles. This thesis aims to use the techniques which were developed in that project to impregnate the fibre bundles with nanometer sized particles.

The main challenge to overcome when spreading the fibre bundles is to avoid damaging them. After reviewing multiple different spreading techniques the previous project judged a spreading technique called pneumatic spreading used by El-Dessouky et al. seemed effective[6]. With this technique the fibre bundle is led over a vacuum using rollers. The suction from the vacuum causes the fibre bundle to momentarily lose tension and the fibres are allowed to spread apart. Thus the fibre bundle is allowed to separate while using a relatively small amount of force and therefore little damage [36].

An open impregnation technique using a bath was implemented in the previous project. The technique was based on work done by Koncherry et al. in 2017 [6]. Via three rollers the fibre bundle can be drawn into a bath with the relevant coating under tension as shown in figure 7. If the middle roller is convex than further spreading can occur in this step allowing for more thorough impregnation [37].

Figure 7: Impregnation of a fibre bundle using an open bath[37]

A combination of spreading and impregnating fibres will be used in this thesis work. By first spreading the fibre bundle and then impregnating it with the desired coating one achieves a good impregnation of the fibre. As previously stated the solgel mixtures were acid catalysed so it was important that the rollers and bath were acid resistant to avoid contaminating the coating.

Another method that was also explored during the course of the thesis work was dip coating. After preparing the solgel mixture the fibre bundle is simply immersed in the solution. While this method does not achieve uniform impregnation it requires minimal set up and is quick to perform. Thus it was used for preliminary studies to evaluate the potential of different recipes.

3 Methods

This section presents the methods used during this project starting with the materials during the projects course. Afterwards a description is given of how the coatings and cements were prepared. Finally the experiments performed to evaluate the coatings are described.

3.1 Materials

All of the chemicals were purchased from Sigma-Aldrich except for sodium hydroxide pellets which were purchased from Scharlau. Four different types of fibre bundles were used in this project which can all be observed in table 1.

Table 1: The different fibre bundles used

Type of Fibre bundle	Manufacturer	Product number
Unsized Carbon	Tenax	IMS65-24K
Sized Carbon	Tenax	UTS563i
Industrial Carbon	Tenax	SITgrid017
Industrial Basalt	US Basalt	US-GRD-25-100

3.2 Solgel Workability

All non-organically modified solgels made during this study were derived from recipes developed by Mcdonagh et al. for solgel coatings on silicon and glass substrates [15]. The first solgels focused on optimizing the recipes in regard to their workability. The different studied recipes can be viewed in table 2. The different pH values were achieved by adding HCl until the values were measured using a Hanna pH meter HI98103. After stirring for one hour at room temperature, the mixtures were left to age at room temperature followed by a 60-65 °C water bath for times seen in table 2.

Table 2: Experiments performed to evaluate the workability of different solgel recipes.

TEOS/EtOH/H2O	pH	ageing time room temperature (h)	ageing time water bath (h)
1/3/3	0,5	20	0
1/5/5	0,4	20	0,33
1/3/3	1	66	1

The times shown in table 2 are the times required until full gelation was observed. With the knowledge that full gelation didn't occur within a handful of hours and the results found by Mcdonagh et al. [15] it was decided upon that the basic inorganic recipe for this thesis work would be a 1/4/4 solgel with no ageing. Mcdonagh found that a water-silica ratio of 4 gave a sol that was coatable after no ageing. Films with a ratio of 4 also remained stable after 100 days and provided thicker coatings than lower ratios [15].

3.3 Dip Coating

To dip coat fibre bundles they were pushed by a nitrile glove covered hand as a coil into the solgel mixture until the entire bundle was wetted. After dipping the fibre bundles were suspended from a stand and the solgel was allowed to harden and dry in an oven at 70°C for at least 24 h. The bundles

that were dip coated and the solgel recipes used are shown in table 3. pH varied between 0,4 and 1,0 and the fibre numbers denote which experiment it was.

Table 3: Inorganic coatings applied unto unsized fibre bundles using dip coating

Fibre	Coating	Ageing (h)
1	TEOS 1/4/4	0
2	TEOS 1/4/4	1
3	TEOS 1/8/4	1
4	TEOS 1/8/4	2
5	TEOS 1/8/4	3
6	TEOS 1/8/4	4
7	TEOS 1/4/4	0

3.4 Spread Coating

To spread carbon fibre bundles under tension an experimentall set up shown in figure 8 was used which is explained with the help of a diagram in figure 9.

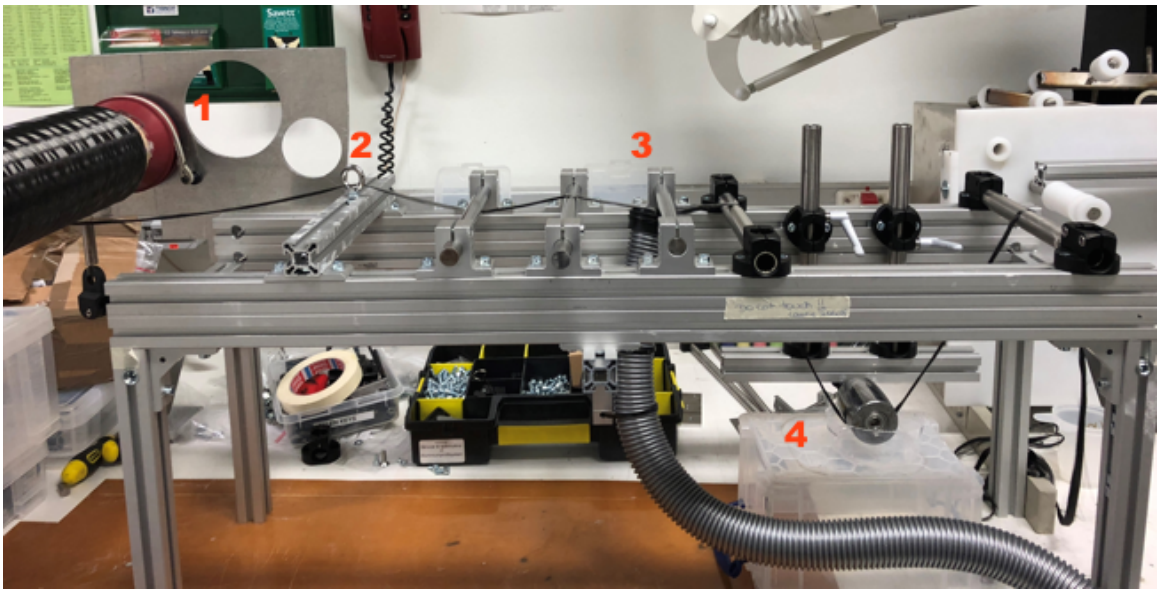

Figure 8: The equipment used to spread fibre bundles. The numbers correspond to 1: the fibre roll, 2 Guiding ring, 3: Vacuum, 4: Coating bath

In the far left of figure 8 one can view the fibre roll marked with the number 1. The fibre bundle is then led through a guiding ring marked 2 to stop the fibre bundle from veering away from the vacuum suction marked 3. Mark 4 denotes the coating bath which is made of teflon with a convex roller submersed in it. Figure 8 also shows clearly how the fibre bundle was kept under tension while being led through the equipment. The fibre bundle was pulled through the equipment and cut after coating by hand.

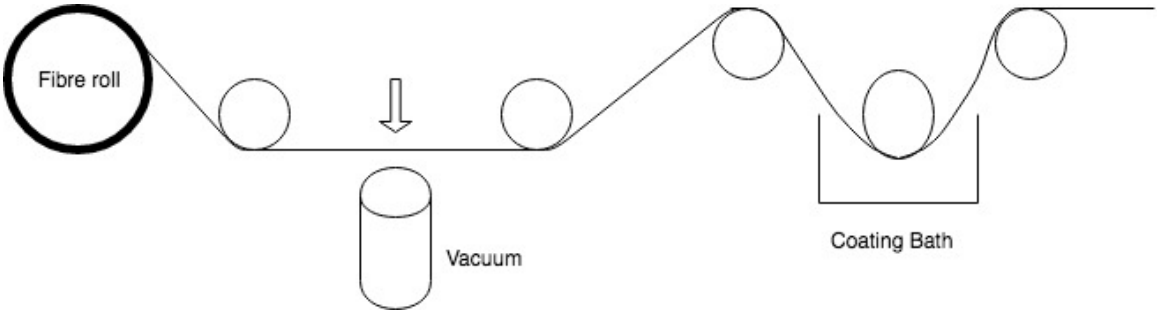

Figure 9: Diagram of the equipment used to spread fibre bundles.

Figure 9 is a schematic overview of figure 8 and show how the placement of the rollers to maintain fibre bundle tension. The first two rollers are used to keep the fibre bundle pressed close up against the vacuum for maximum effect. The other three rollers are situated in such a way to increase the tension while the fibre bundle is impregnated in the bath. The roller that is partially submersed in the coating bath is shown as slightly oval because it is convex, which achieves additional spreading.

Two different kinds of coatings and two different kinds of fibre bundles were spread and impregnated with this method. Unsized carbon fibre bundles were coated with both inorganic TEOS coatings and Ormosil TEOS coatings modified with GLYMO or VTMOS. Sized carbon fibre bundles were coated with the Ormosil coatings.

3.4.1 Unsized Carbon fibre bundles

The inorganic TEOS coatings recipes can be seen in table 4. No ageing was performed before curing and pH varied between 0,6 and 1. After the fibre bundles were impregnated they were suspended from a stand and dried in an oven for at least 24 hours at 70°C.

Table 4: Inorganic coatings applied unto unsized fibre bundles using spreading coating

Fibre	Coating	Ageing (h)
8	TEOS 1/4/4	0
25	TEOS 1/4/4	0

The Ormosil coatings were derived from recipes developed by Metroke et al. [38][30]. The TEOS solgels were modified with either GLYMO, (3-Glycidyloxypropyl)trimethoxysilane, or VTMOS, Vinyltrimethoxysilane. The GLYMO coatings consisted of 5,5 ml TEOS, 1,84 ml GLYMO, 3,3 ml 0,05 M HNO_3, and 0,05 ml H_2O. The VTMOS coatings consisted of 2,24 ml TEOS, 3,92 0,05 M HNO_3, 3,04 VTMOS and 0,84 ml MEMO, 3-(Trimethoxysilyl)propyl methacrylate. To some VTMOS coatings one or two ml of PTMOS, trimethoxy(propyl)silane were added. An overview of the Ormosil recipes used can be seen in table refGLYMO. After the fibre bundles were impregnated they were suspended from a stand and dried in an oven for at least 24 hours at 70°C.

3.4.2 Sized Carbon Fibre Bundles

Spread coating was also used to impregnate sized carbon fibre bundles. These were coated using the VTMOS and GLYMO recipes which were presented in the previous section. There was no PTMOS

Table 5: Ormosil coatings applied unto unsized fibre bundles using spread coating

Fibre	Coating	Ageing (h)
9	GLYMO	0
10	VTMOS	0
11	VTMOS	1
12	VTMOS + 2 ml PTMOS	0
13	VTMOS + 2 ml PTMOS	1
14	VTMOS + 1 ml PTMOS	0
15	VTMOS + 1 ml PTMOS	1
16	VTMOS + 1 ml PTMOS	2

added to the VTMOS coatings. An overview of the different coatings that were prepared can be seen in table 6

Table 6: Ormosil coatings applied unto sized fibre bundles using spread coating

Fibre	Coating	Ageing at room temperature (h)
19	GLYMO	1
20	GLYMO	2
21	VTMOS	0
22	VTMOS	1

3.5 Industrial Reinforcements

A series of tests were also performed on fibre bundles which are used in the industry today, one carbon and one basalt. These were used as they were delivered and were not spread or impregnated. Each fibre bundle had to be removed from the grids shown in figure 10 by hand to test a single fibre bundle.

3.5.1 Plasma treatment

Some industrial reinforcements were plasma treated before further testing to see if increasing the oxidation of the fibre bundle would increase adhesion. Plasma treatment was performed in a vacuum plasma chamber (440 Plasma System, Technics Plasma GmbH, Germany) in the presence of oxygen gas. All plasma treatments were performed at an oxygen gas pressure of 0.7mbar and a plasma power of 320W for 1 minute.

3.6 Development of cement

The production of cement went through multiple stages during this project. At first cements were made by mixing 32,5 g of water glass and 50 g of slag cement. The water glass had a modulus of 1,2 and a solid content of 18%. The slag cement consisted of 19,25g slag, 4,8g portland cement, 0,95g gypsum and 25g fine sand. At later stages in the project an additional 50g of 0-0,4 mm sand was added to this recipe. After mixing the cement impregnated fibre bundles were immediately inserted while it was still liquid and held in place during the initial hardening.

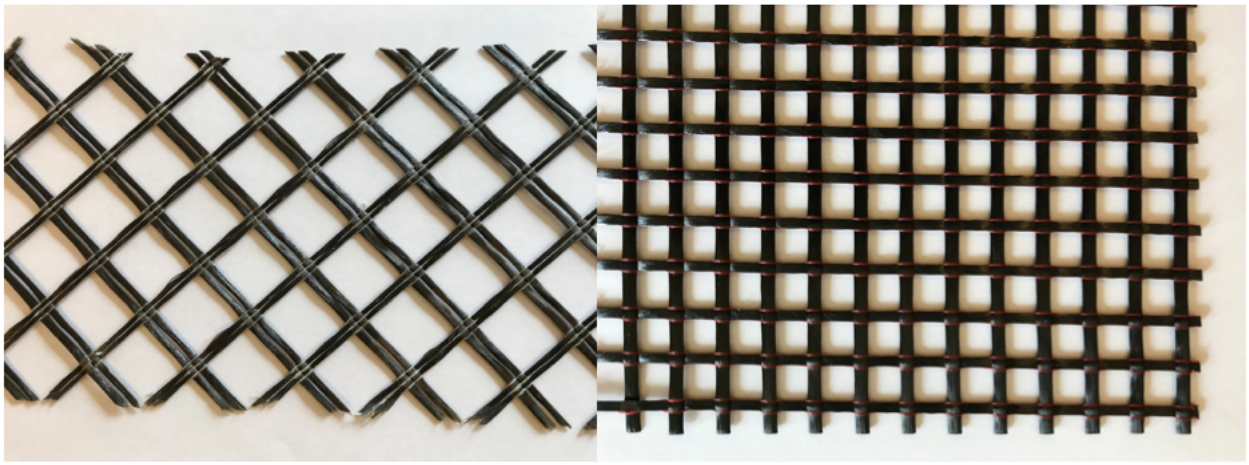

Figure 10: The grids from which industrial reinforcements were removed. To the left the basalt reinforcements and to the right the carbon reinforcements

To reduce cracking while drying the cements were moved to a water bath after at least 30 minutes of hardening. This was done either by embedding a wooden stick into the cement or by removing a paper mould after at least 30 minutes of curing. After having been moved to a water bath they were left to cure for at least 72 hours. How the cements were placed in the waterbaths is shown in figure 11.

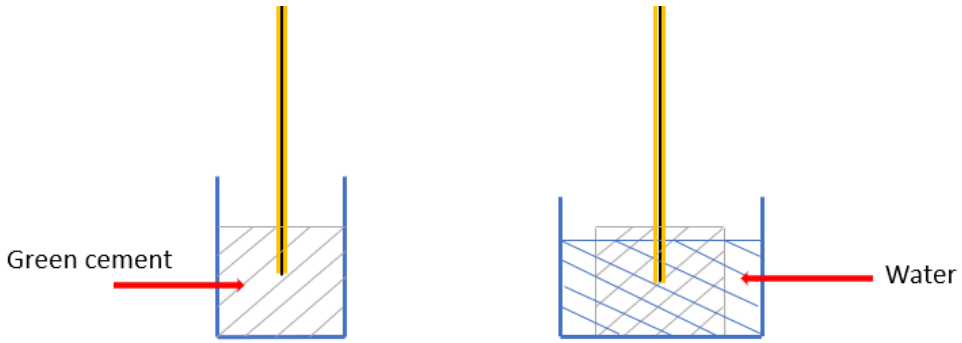

Figure 11: The way cement samples were submersed in water after hardening.

Important to note in figure 11 is that no water makes contact with the carbon fibre bundle and the water level stays under the top of the cement sample. One experiment was not embedded into cement but into concrete, specifically ”RAW finbetong”, which was not moved to a water bath.

3.7 Pullout Testing

All fibre bundles that were embedded into cement had their maximum pullout strength tested. The pullout strength of the fibre bundles were tested using an AG-XK plus Shimadzu with a 50 kN grip at a speed of 1 mm/min. The set up used to place the samples in the machine is shown below in

figure 12. A rubber material was placed between the grips and the cement to prevent contact stress. If the pullout strength required was less than 5 N it did not register.

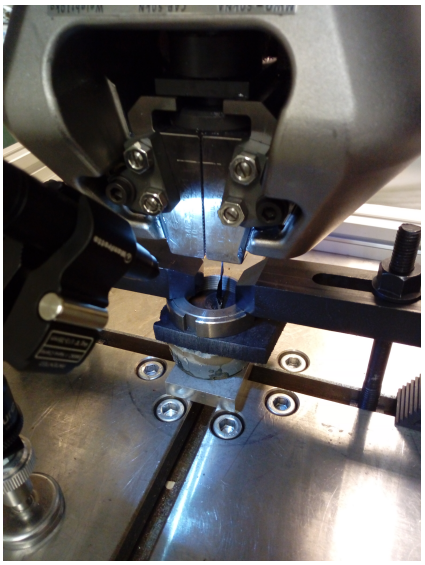

Figure 12: The set up used to test the pullout strength of samples

To reduce slippage fibre bundles were held between two tabs with p800 sandpaper glued to them when placed into the grip.

Using a perimeter found via microscopy the following equation, based on findings in literature, was used to calculate shear stress, τ [39].

$$\tau = F/(P * H) \tag{2}$$

In equation 2 τ is interfacial shear strength, F is maximum pullout load, P is the perimeter of the embedded fibre bundle, and H is the embedded length.

3.8 Optical Microscopy

A selection of fibre bundles with high pullout strengths were examined under an Olympus BH2-UMA Universal Vertical Ilumminator to examine the impregnation quality and to perform a perimeter analysis which is required for calcuation of the interfacial shear strength. The impregnated fibre bundles were cut and cast into a mix an Epofix Resin and EpoFix Hardener. The resin was mixed by hand for 1 minute, the bundles were then placed vertically in the mixture and each mixture was place in vacuum for 20 minutes before being left to cure for 24h in ambient conditions. Thereafter each epoxy puck was grinded down using a Struers Tegramin-30. The grinding papers were used in decreasing grain size P500, P1200, P2000, and P4000. Finally the samples were polished in the same machine using MD Dur polishing paper with a Diapro Dac 3 suspension with a 3μm particle size.

Some fibre bundles were examined further under a Lietz Aristotmet Optical Microscope which gave the possibility of using flourescent light. In order to ensure that the fibre bundles are exposed at the surface of the puck, the bundles were placed in the holder so that a portion of the bundles was above the epoxy surface. This portion was removed after hardening.

If the fibre bundle had been pullout tested before being examined with microscopy the segment that was cast into epoxy came from inbetween the pullout grip and the cement puck. This was to avoid interference in the image due to damage by friction and cement residue in the fibre bundle.

3.9 Strength of the Fibre Bundle

Three tests were performed to test the strength of the unsized fibre bundle. p800 sandpaper was glued onto three sets of tabs. By fastening both ends of the fibre into a grip in the shimadzu machine the strength of the fibre could be tested. One set of tabs was covered in cyanoacrylate, another in epoxy, and the third was left with just the sandpaper.

4 Results and Discussion

All of the results are presented in this section along with a discussion of the interpretation of those results. The coatings which coated embedded carbon fibre bundles are evaluated and compared to their industrial counterparts. This is explained using two different methods first microscopy followed by a calculation of their interfacial shear strength. Because not every fibre bundle was examined under a microscope a complete overview of every fibre bundle that was embedded into cement is not given until the later section. The final two sections discuss how the quality of the cement and the strength of the fibre bundle effected the interfacial shear strength measurements.

4.1 Microscopy

Microscopy was performed with two goals in mind, examining the degree of impregnation and performing a perimeter analysis, which is required for the calculation of the interfacial shear strength. The images which were used to perform the perimeter analyses are shown below. They were stitched together from a series of of images to show a cross section of the fibre bundle.

The fibre bundles which are shown below are all numbered according to a system described in a later section 4.2. The perimeters which are found in this section will be used there to calculate interfacial shear strength (ISS). The ratios shown in the titles of some subsections are the ratios between TEOS/EtOH/H_2O.

4.1.1 Cohesive Fibre Bundles

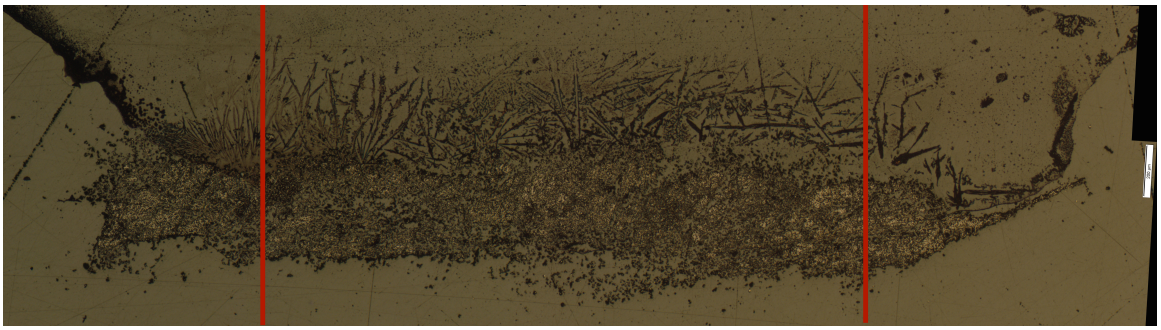

Figure 13: Fibre bundle 8a magnified 5 times

8a, whose coating described below in table 7 and was spread coated, had a perimeter of 8,54 mm. A relative uniformity can be observed in figure 13. Even though it was difficult to distinguish between coating and fibre the fact that the entire fibre bundle is cohesive suggests that the impregnation was successful. On the left hand side of the figure a dark streak can be seen which was assumed to be an air bubble or other defect in the epoxy. The streaks above the fibre bundle were also assumed to be defects in the epoxy. These areas were carefully examined when performing the perimeter analysis to avoid the inclusion of the defects. To confirm the assumption that they were defects images were taken using a fluorescent microscope resulting in figure 14. The red lines in figure 13 represent the left and the right side of the image shown below in figure 14

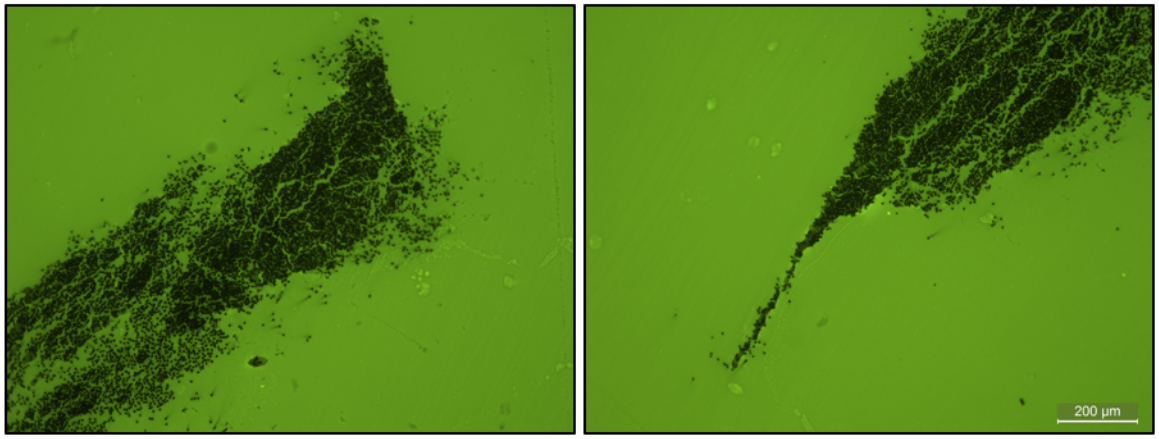

Figure 14: The ends of fibre bundle 8a magnified 5 times under a fluorescent microscope.

To ease viewing the left image of figure 14 shows the left end of figure 13 and vice versa even though they are rotated. As figure 14 clearly shows the epoxy resin is fluorescent which makes it easier to distinguish between fibre and epoxy. The defects do not appear because they are not visible when the light is fluorescent. Which makes it clear that they were indeed defects and not something else.

It is also possible to view the extent of impregnation in figure 14. Each circular black fibre has a darkened green area around it. The coating is partially transparent and therefore some fluorescence shines through it but blocks it partially. Therefore closely packed fibres appear more coated because more light is blocked out. Of particular note is the thin line of fibres in the right hand image. Even though it at some points is no more than 4 fibres across there is still enough coating to be viewed clearly.

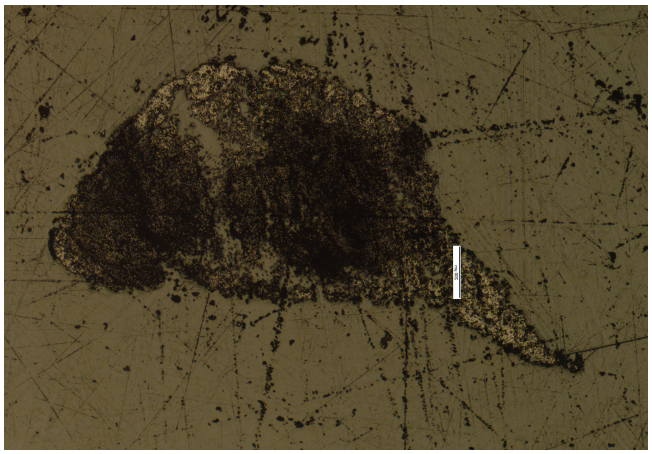

Figure 15: Fibre bundle 25b magnified 5 times

25b, whose coating is described below in table 7 and was spread coated, had a perimeter of 5,769 mm however as can be seen in figure 15 the impregnation quality was different from 8a. Besides the fact that the fibre bundle has a much smaller perimeter there are also large dark areas. The smaller perimeter is seen as a result of natural variation because the coating process is performed by hand. The darker areas could either be epoxy defects as in 8a, areas where impregnation was poor, or places where the impregnation is thorough and the fibres are densely packed and no light can pass through.

To examine the impregnation quality, 25b was also subjected to a flourescent microscope and the images can be seen in figure 16

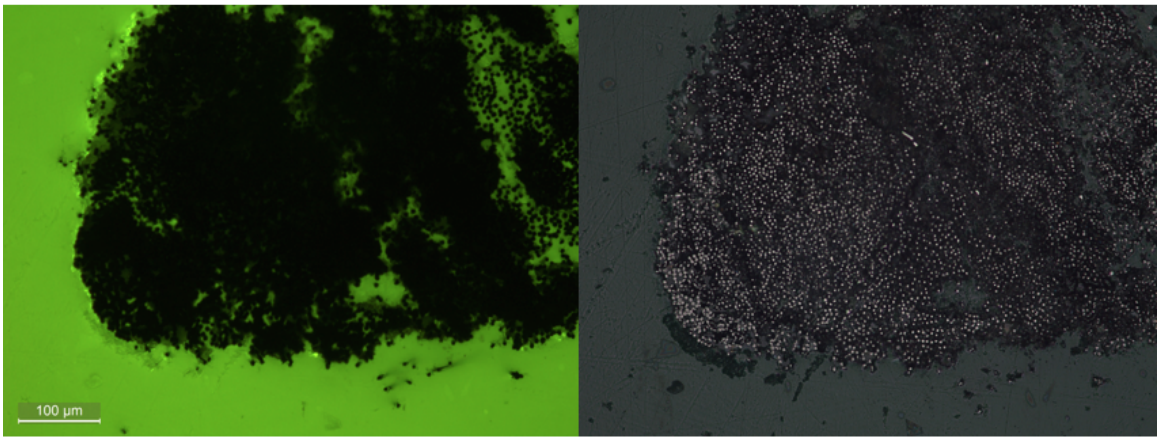

Figure 16: Fibre bundle 2b magnified 10 times. Left: fluorescent light, right: visible light

The fluorescent image on the left of figure 16 clearly shows that there is little epoxy in between the fibres. In the right image one can make out that there is spacing in between the fibres suggesting that it is coating that blocks out light from the epoxy and not densely packed fibres. To get a closer look at the coating a more magnified version of the right image is shown in figure 17

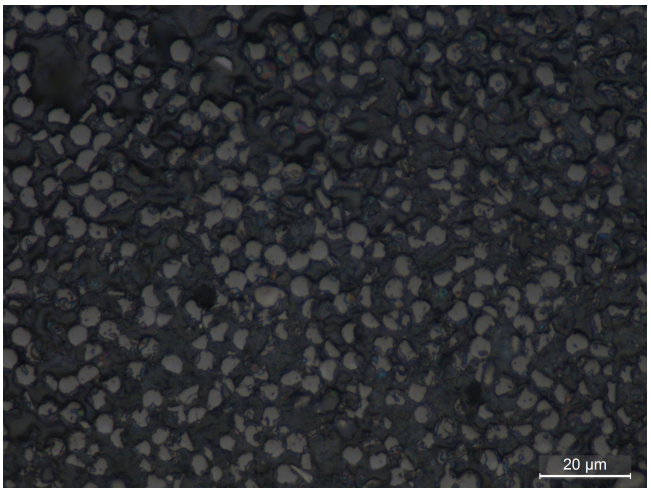

Figure 17: Fibre bundle 25b magnified 50 times

Figure 17 clearly shows that the fibres are impregnated well in the darker areas of the flourescent image in figure 16. The white circles are assumed to be light reflecting off of the carbon fibres.

4.1.2 Industrial Reinforcements

In order to allow comparison of the interfacial shear strength of the fibre bundles coated in this thesis with industrial reinforcements, the perimeter of the industrial reinforcements was measured. The carbon fibre bundle 23b had a perimeter of 9,164 mm. The basalt fibre bundle 24a had a perimeter of 6,059mm. The images used to calculate the perimeters are shown in figures 18 and 19.

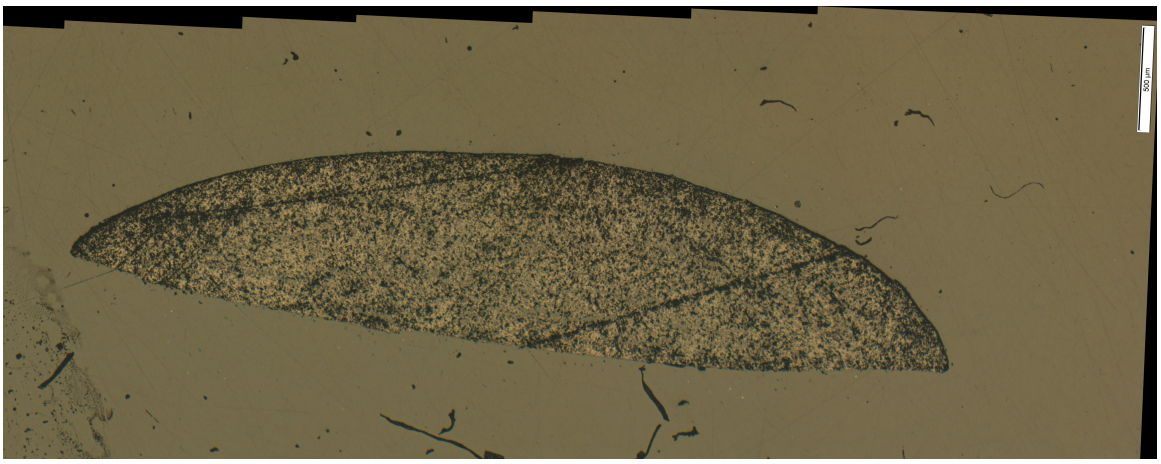

Figure 18: Fibre bundle 23b magnified 2 times

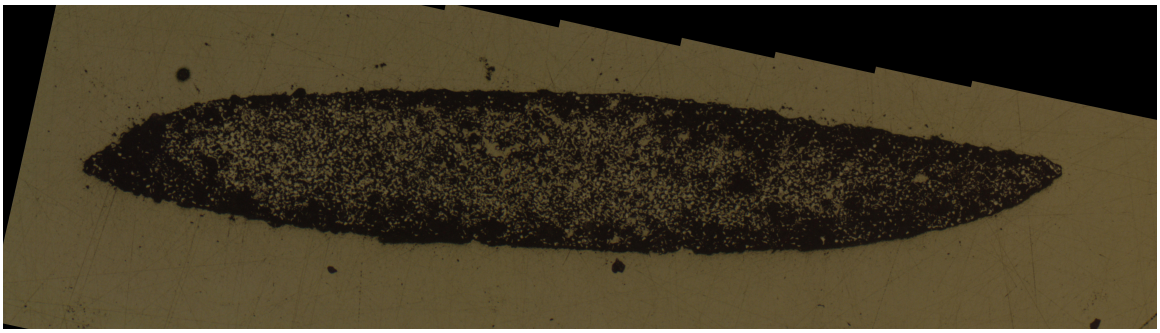

Figure 19: Fibre bundle 24a magnified 5 times

4.1.3 Non cohesive fibres

Two fibres were examined under a microscope and it was not possible to perform a perimeter analysis because the fibres were not cohesive. One was a dip coated, fibre 4, and another was a fibre spread coated with the same coating as 8a but was never subjected to a pullout test.

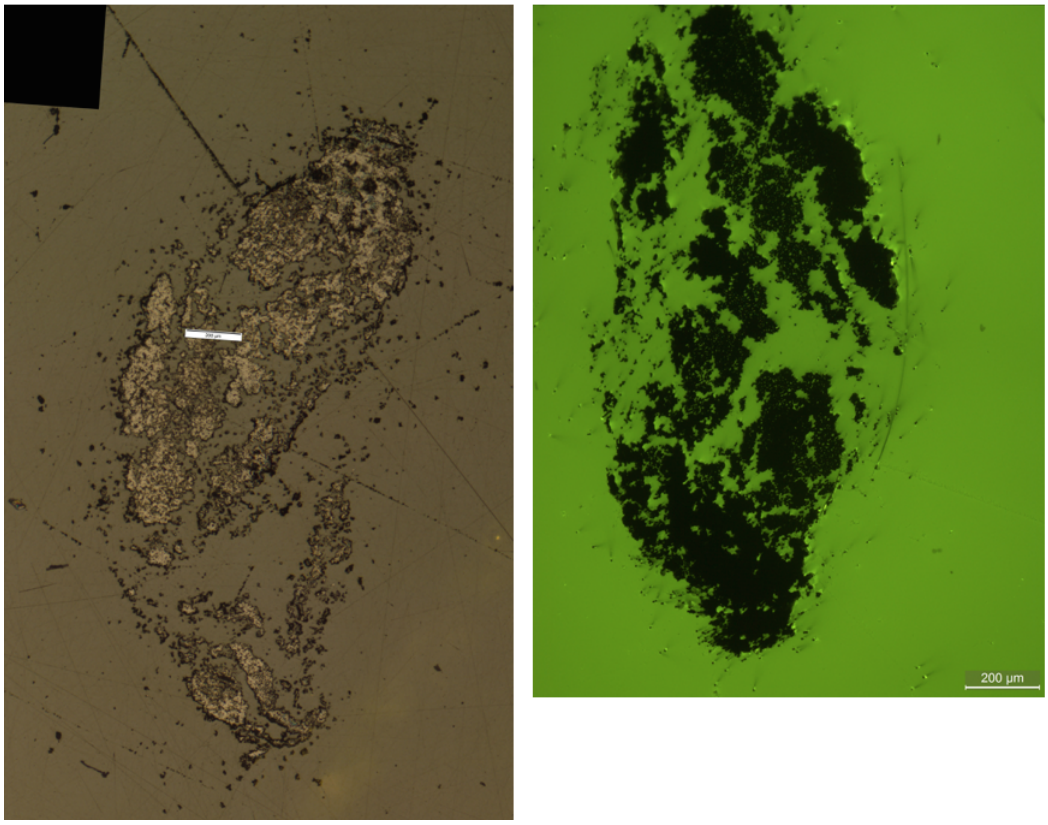

Figure 20: Fibre 4 magnified 5 times Left: visible light, right :fluorescent light

Figure 20 shows the microscopy of the dip coated fibre bundle 4 whose coating described below in table 7. Figure 20 clearly shows why it was difficult to perform a perimeter analysis, there is no clear perimeter. It is impossible to know if cement was inbetween each fibre bundle or not. What is clear from figure 20 is that the different impregnation techniques had a clear impact. The spread coating technique gave a more homogeneous coating.

Fibre 8a was embedded into epoxy at two different points during the project. Above in figure 13 the fibre was embedded into epoxy five months after the pullout test was performed. Below are images taken of the same coating but it was embedded into epoxy directly after coating and this sample was never subjected to pullout testing. Figure 21 shows three different segments of the fibre that was embedded into epoxy directly.

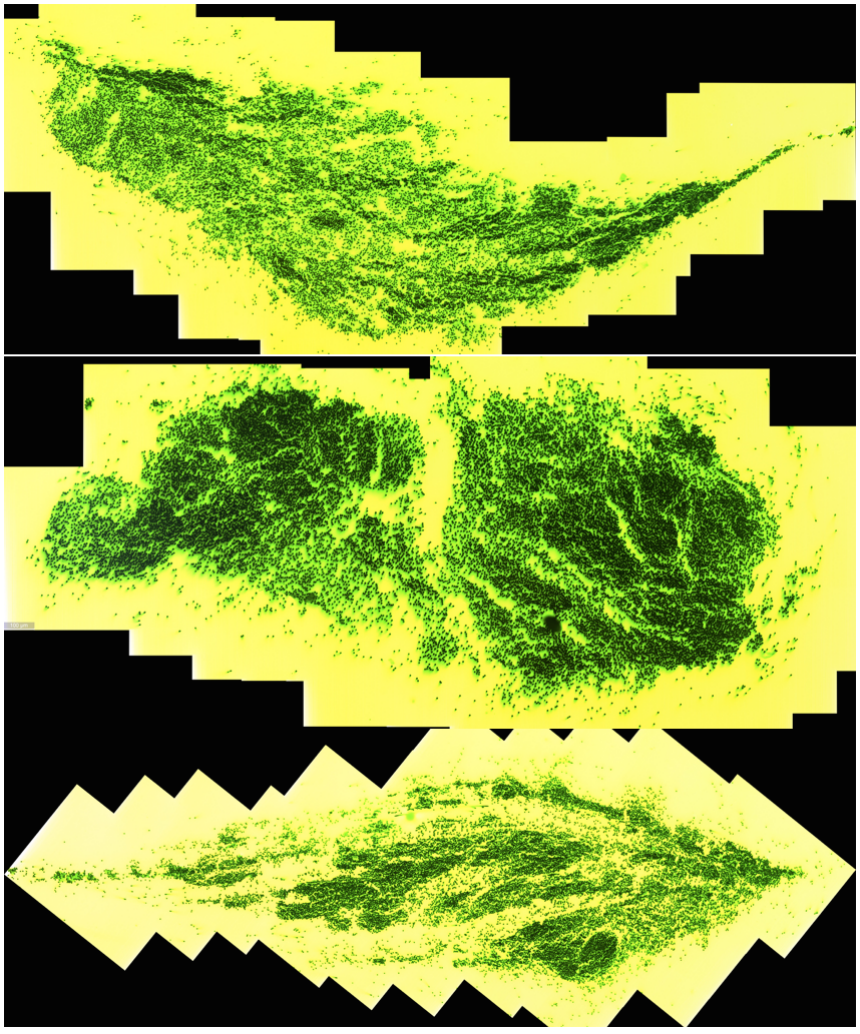

Figure 21: Three different segments of fibre 8a which were embedded into epoxy directly after coating magnified 5 times.

Because figure 21 shows three different segments of the same fibre bundle and it clearly indicates that the process is not consistent. The level of impregnation is different for each fibre and the perimeter while impossible to calculate is clearly a different size for each fibre bundle segment.

When comparing figure 21 with figure 13 one notices that figure 13 has a more cohesive perimeter while the other does not. The only difference between the two is that the latter was stored for 5 months and was subjected to pullout testing. Storage if nothing else should have worsened the cohesiveness of the fibre and not improved it because it inorganic coatings are brittle. During pullout testing the fibre could have been stretched and the fibre bundle could have become more cohesive during that point. If this is true it calls into question the accuracy of all perimeter calculations. However because all fibres were subjected to the same method it is still a useful tool for comparison.

The comparison of the two fibre bundles suggests that inorganic coating degradation is not very high. While it is not possible to calculate that exact amount of coating both before and after the 5 months of storage what is clear is that both fibres are still coated.

4.2 Interfacial Shear Strength

56 coated fibre bundles were embedded into cement and pullout tested over the course of this project. The perimeter which were presented in section 4.1 were used to calculate interfacial shear strength (ISS). The smallest perimeter of any fibre bundle was that of 25b with a perimeter of 5,77mm. This perimeter was used to find the potential best case scenario interfacial shear strength for each individual fibre bundle using equation 2.

Below a series of tables are shown with the results from the pullout tests, with each coating being denoted with a number. If the same coating was tested multiple times then a letter is seen after the number. Because the goal of this thesis is to show the potential of different coatings, when a coating was tested multiple times only the maximum pullout strength is shown which was in turn used to calculate the interfacial shear strength. The parameters that could influence the measured pull-out strength, such as poor concrete quality or poor impregnation, will lead to a lower measured pull-out strength. This means, that the highest measured value describes the potential pull-out strength in case of optimized impregnation and cement quality. The calculated interfacial shear strengths are calculated using the perimeters given specifically for that fibre shown in section 4.1

4.2.1 Inorganic Coatings

The variables that were changed for inorganic coatings were pH and TEOS/EtOH/H_2O ratio. pH varied between 0,5 and 1. The results from pullout testing of the inorganically coated fibre bundles can be seen in table 7.

Table 7: An overview of the calculated (calc.) and potential (pot.) interfacial shear strength of all inorganic coatings

Fiber	Max pullout (N)	Calc. ISS (N/mm^2)	Pot. ISS (N/mm^2)	Coating	Ageing (h)
1	18,24		0,14	TEOS 1/4/4	0
2	68,86		0,52	TEOS 1/4/4	1
3	66,1		0,50	TEOS 1/8/4	1
4	266,06		2,01	TEOS 1/8/4	2
5	171,82		1,29	TEOS 1/8/4	3
6	89,4		0,67	TEOS 1/8/4	4
7	29,92		0,23	TEOS 1/4/4	0
8a	239,91	1,17	1,73	TEOS 1/4/4	0
8b	134,14		0,97	TEOS 1/4/4	0
25a-c	114,40	0,83	0,83	TEOS 1/4/4	0

While table 7 gives a good overview of the quantative data however some additional data is required to draw conclusions from the experiments. 8a was the first experiment to use the full method for making cement and was also the first not to show any signs of cracking. 1 and 2 were not moved to water baths and it was not until 7 that paper moulds were introduced. This led to the cements of 2, 3, and 4 to fail and break where the fibre bundle was embedded. 8a was also the first fibre bundle to be spread coated instead of dip coated.

In theory 8a and 25a-c were made with a superior method and should therefore exhibit stronger interfaces than the other experiments. This is true for all experiments except for experiments 4 and 5 according the potential ISS. It should be taken into account though that the potential ISS is a best case scenario and not necessarily a reflection of what happened in reality. This can be clearly seen in the large difference between the calculated and potential ISS of 8a. However 4's cement broke apart and potentially the ISS could have been even higher if the cement was of a higher quality. Fibre bundle 4 was also seen sticking to the cement surface as can be observed in figure 22.

Figure 22: Experiment 4 after pullout

There were other experiments which also had fibre strands left in the cement puck in a similar fashion to 4. While they did so in varying degrees it is possible that the shear strength could have been increased if the the fibre integrity was higher. The unsized fibre bundles used were generally weaker because the fibres are not able to distribute stress as easily. The experiments where fibre strands were left on the cement were 4, 5, 6, 13a, and 16c.

One test was also performed to test the quality of green cement and a single fibre bundle was embedded into concrete (RAW finbetong). That fibre bundle was 8b and it performed comparatively well to 8a and other inorganically coated fibres.

4.2.2 Ormosil Coatings

The variables that were changed for the Ormosil coatings were the recipe and ageing time. An overview of the results from the pullout testing is seen in table 8. The fibre bundles 19 through 22 were sized. Many of the fibre bundles were tested multiple times increasing the statistical validity of these results. As stated earlier only the best result from each test is shown.

Table 8: An overview of the estimated interfacial shear strength of all Ormosil coatings

Fiber	Max pullout (N)	Potential ISS (N/mm^2)	Coating	Ageing (h)
9	61,17	0,44	GLYMO	0
10	51,85	0,37	VTMOS	0
11a-b	28,37	0,20	VTMOS	1
12	14,76	0,11	VTMOS + 2 ml PTMOS	0
13a-b	6,48	0,05	VTMOS + 2 ml PTMOS	1
14a-c	14,82	0,11	VTMOS + 1 ml PTMOS	0
15a-c	20,84	0,15	VTMOS + 1 ml PTMOS	1
16a-c	53,71	0,39	VTMOS + 1 ml PTMOS	2
17a-c	40,44	0,29	GLYMO	2
18a-c	24,41	0,18	GLYMO	3
19a-c	6,63	0,05	VTMOS	1
20a-c	18,97	0,14	VTMOS	0
21a-c	23,13	0,17	GLYMO	1
22a-c	no reading	N/A	GLYMO	2

No Ormosil coated fibre bundles were examined under a microscope. This was because not one resulted in a particularly high pull out strength. Even the potential ISS which is seen as a best case scenario was at its highest 0,44 N/mm ^{2}. There were only two organic coatings which performed worse and both of those experiments had cracked cements. It is likely that the organic precursor added irregularities to the polymer network. This would decrease the overall strength of the coating and decrease integration with the cement.

While the goal was to increase bonding to the fibre bundle without some form of surface treatment of the fibre it seems unlikely that this took place or if it had then the bonding to the cement was weakened to such an extent that it was not valuable. Even the sized fibre bundles were not able to make a more successful bond to the Ormosil coatings.

It should be noted that the fact that fibre bundle 22 gave no reading is likely due to cement failure and not due to the coating. Holes were found in the bottom of the cements where water was allowed to come into contact with the fibre bundle.

4.2.3 Industrial Reinforcments

The industrial reinforcements were mainly tested to compare to the coated fibre bundles however a test was also performed to test the effectiveness of plasma treatment. The results of these tests can be seen in table 9.

Table 9: An overview of the calculated interfacial shear strength of industrial reinforcement

Fiber	Material	Plasma Treatment	Max pullout (N)	Calculated ISS (N/mm^2)
23a-c	Carbon	No	251,96	1,15
24a-c	Basalt	No	114,43	0,79
26a-c	Carbon	Yes	261,75	1.54
27a-c	Basalt	Yes	258,96	2.38

An increase can be seen of ISS after plasma treatment. This suggests that bonding to a silica network increases after plasma treatment.

4.2.4 Comparison of Coatings

The industrial reinforcements had interfacial shear strengths of 1,15 and 0,79 N/mm^2. There were two impregnated fibre bundles which performed better than their industrial counterparts based on their calculated shear strength. 25 with 0,83 N/mm^2 and 8a with 1,73 N/mm^2. If the potential ISS is taken into account then two more fibres bundles perform better, 4 and 5.

A visual comparison of the of the highest performance of each type of coating as well as the industrial reinforcements is seen below in figure 23.

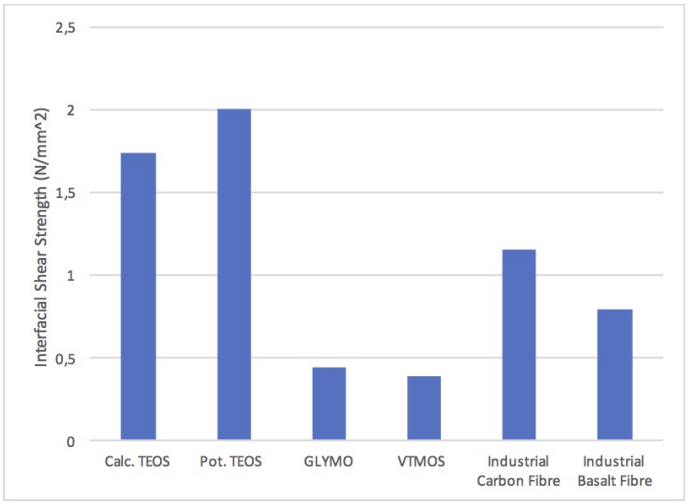

Figure 23: A comparison of the ISS of different types of coatings as well as the industrial Reinforcements

The TEOS coatings can clearly perform better their industrial counterparts. The potential ISS for a TEOS coating is almost twice as strong as the industrial carbon reinforcement and the calculated is still stronger by a large margin. The GLYMO and VTMOS coatings did not perform particularly well and as stated before they are both potential ISS and not calculated.

The method used to make the coatings in this project lack precision. Almost every step is performed by hand. As can be seen in section 4.1 the same fibre coating made using the same method can vary widely. This was also observed during pullout testing. For a single coating there could be a variation of as large as 90 N of max pullout strength. The fact that even with this imprecise and non refined method results it was still possible to produce results which performed better than their industrial counterparts speaks to the potential of using solgel as a coating.

4.3 Cement Quality

While difficult to evaluate quantitatively the quality of cement used effected the interfacial shear strength of many experiments. Of the 56 fibre bundles which were embedded two had cements that clearly failed before the max pullout strength was reached. Fibre was still stuck to the surface even though the cement broke apart. Two other cements also broke apart around the embedded fibre bundle but no trace of fibre was found afterwards. For three of these four failures the cement recipe had not been finalized yet and extra sand had not been added. The fourth was removed from its paper mould too quickly and was not cured properly.

In the bottom of 11 cements water was able to come into contact with the fibre bundles because of holes in the bottom of the cement. When this happened to only one test which was repeated it was clear that the pullout strength was greatly reduced. All three fibre bundles with coating 22 showed a hole in the bottom and none registered a pullout strength. Aside from coating 22 all the other 11 at least one result which did not have a defect.

One important fact to note is that the industrial reinforcements were embedded into cements which exhibited no defects. As a control for the other experiments it seems that the role was fulfilled. While other cements failed there were a few which performed well in comparison to the industrial reinforcements.

4.4 Solgel Degradation

All fibres were vertical after curing which suggests that the coating had not dissolved or at least the area right under the cement surface had not dissolved. However there were multiple fibres which had lost stiffness after the pullout test. If dissolution had not occurred than it is likely that is was removed physically during the pullout test. Especially the inorganic coatings could be easily removed and were brittle. After a series of tests it was noticed that the coating could be removed by hand.

To increase the robustness of the coating the Ormosil coatings were developed. The first tests which were not embedded clearly showed that the coatings were less brittle which confirms what was theorized in section 2.4. It was not possible to remove the coating by hand and more force was necessary to bend the fibre.

4.5 Strength of Fibre bundle

Multiple times parts of the fibre bundles were left inside the puck. In these cases the question arises if it was the shear forces against the cement that failed or the fibre itself that was pulled apart. An initial attempt was made to place just a carbon fibre bundle in tabs and try to pull it apart to test the tensile strength. This resulted in the fibre bundle slipping in the tab and no read out was given.

In attempt to reduce slippage the tabs were glued to the fibre bundle. One with epoxy and one with cyanoacrylat. After drying however it was noted the that the entire fibre bundle was impregnated with the glue as it had traveled through capillary forces through the fibre. This improved the tensile strength greatly but did not prove the strength of the fibre bundle with other coatings. The epoxy resulted in a tensile strength of 580 N and the cyanoacrylate 1246 N.

5 Conclusion

The aim of this project was to find the potential of solgel coatings not definitively find a coating which has a higher shear strength than what is used in the industry today. With that in mind there are several which performed well enough to warrant further examination in future studies. However as has been shown above it is not possible to say that any solgels are definitely better than their industrial counterparts because of the large variations between tests.

The inorganic coatings performed far and away the best out of all the coatings that were tested. However only 1/4/4 coatings had a clear enough perimeter to be measured. While the two different 1/4/4 coatings did perform better than their industrial counterparts they were not the ones with the highest pullout strength. Indeed some 1/8/4 had higher pullout strengths even though they were dip coated and had inferior cements. If a more refined method, with more consistent results, is developed the most interesting coatings to examine further would be 1/8/4 with 2 or 3 hours of ageing and 1/4/4 with no ageing.

The ormosil coatings were less promising than their purely inorganic counterparts however there were many factors which were not explored. The extent to which the coatings were organically modified or incorporating other organic substrates are possibilities. The ormosil coatings that were tested however did not perform well enough to warrant pursuing a refinement of those coatings. Instead the potential of different ormosils should continue to be tested.

Finally this thesis can conclude that what is used in the industry today does not provide the highest shear strength. While many other aspects such as cost, lifetime degradation, and scalability were outside of the scope of this project the results that are shown are promising. If future studies refine the method used and explore these other aspects it is possible that the future of TRC's lies in solgel coatings.

Bibliography

(1) Crow, J. M. The Conrete Conundrum. *Chemistry World* **2008**.

(2) Survey, U. G. Cement production globally and in the U.S. from 2010 to 2017 (in million metric tons)., 2018.

(3) Dezem, V. Cement Produces More Pollution Than All the Trucks in the World. *Bloomberg* **2019**.

(4) Miron, L. E.R. D.; Koleva, D. A., *Concrete Durability - 2017*; Springer International Publishing: 2017.

(5) Peled, A.; Bentur, A.; Mobasher, B., *Textile Reinforced Conrcete*; CRC Press Taylor & Francis group: 2017.

(6) Domergue, A. Development of Novel Concrete Reinforcements Based on Carbon Fibres.

(7) Portal, N. W. Usability of Textile Reinforced Concrete: Structural Performance, Durability and Sustainability., Ph.D. Thesis, Chalmers University of Technology.

(8) Fraas, V. 3D textile-reinforced concrete façade elements of only 3-cm thickness. *BFT international* **2012**.

(9) Gupta, R. Surface Treatment for Concrete Reinforcement., 2014.

(10) Hull, D.; Clyne, T., *An Introduction to Composite Materials*; Cambridge University Press: 1996.

(11) Dislich, H.; Hinz, P. History and principles of the sol-gel process, and some new multicomponent oxide coatings. *Journal of Non-Crystalline Solids* **1982**, *48*, Proceedings of the International Workshop on Glasses and Glass Ceramics from Gels, 11 –16.

(12) Colleoni, C.; Esposito, S; Grasso, R.; Gulino, M.; Musumeci, F.; Romeli, D.; Rosace, G.; Salesi, G; Scordino, A. Delayed luminescence induced by complex domains in water and in aqueous solutions. **2014**.

(13) Brinker, C. J.; Scherer, G. W. In *Sol-Gel Science*, Brinker, C. J., Scherer, G. W., Eds.; Academic Press: San Diego, 1990, pp 96 –233.

(14) Hench, L. L.; West, J. K. The sol-gel process. *Chemical reviews* **1990**, *90*, 33–72.

(15) McDonagh, C.; Sheridan, F.; Butler, T.; MacCraith, B. Characterisation of sol-gel-derived silica films. *Journal of Non-Crystalline Solids* **1996**, *194*, 72 –77.

(16) Jiang, M.; Chen, X.; Rajabipour, F.; Hendrickson, C. T. Comparative Life Cycle Assessment of Conventional, Glass Powder, and Alkali-Activated Slag Concrete and Mortar. *Journal of Infrastructure Systems* **2014**, *20*, 04014020.

(17) Puertas, F.; González-Fonteboa, B.; González-Taboada, I.; Alonso, M.; Torres-Carrasco, M.; Rojo, G.; Martínez-Abella, F. Alkali-activated slag concrete: Fresh and hardened behaviour. *Cement and Concrete Composites* **2018**, *85*, 22 –31.

(18) Naqi, A.; Jang, J. G. Recent Progress in Green Cement Technology Utilizing Low-Carbon Emission Fuels and Raw Materials: A Review. *Sustainability* **2019**, *11*.

(19) Association, N. S. Common Uses for Slag., 2013.

(20) Mao-chieh Chi, J.-j. C.; Huang, R. Strength and Drying Shrinkage of Alkali-Activated Slag Paste and Mortar. *Advances in Civil Engineering* **2012**, *2012*.

(21) Valipour, M.; Khayat, K. H. Coupled effect of shrinkage-mitigating admixtures and saturated lightweight sand on shrinkage of UHPC for overlay applications. *Construction and Building Materials* **2018**, *184*, 320 –329.

(22) Garcia-Lodeiro, I.; Palomo, A.; Fernández-Jiménez, A. In *Handbook of Alkali-Activated Cements, Mortars and Concretes*, Pacheco-Torgal, F., Labrincha, J., Leonelli, C., Palomo, A., Chindaprasirt, P., Eds.; Woodhead Publishing: Oxford, 2015, pp 19 –47.

(23) Garside, M. Major countries in worldwide cement production from 2014 to 2018 (in million metric tons)., 2019.

(24) Li, G.; Guo, M. Current Development of Slag Valorisation in China. *Waste and Biomass Valorization* **2014**, *5*, 317–325.

(25) Wu, G.; Ma, L.; Jiang, H.; Liu, L.; Huang, Y. Improving the interfacial strength of silicone resin composites by chemically grafting silica nanoparticles on carbon fiber. *Composites Science and Technology* **2017**, *153*, 160 –167.

(26) Lei, D.-Y.; Guo, L.-P.; Sun, W.; Liu, J.; Shu, X.; Guo, X.-L. A new dispersing method on silica fume and its influence on the performance of cement-based materials. *Construction and Building Materials* **2016**, *115*, 716 –726.

(27) Singh, L. P.; Bhattacharyya, S. K.; Kumar, R.; Mishra, G.; Sharma, U.; Singh, G.; Ahalawat, S. Sol-Gel processing of silica nanoparticles and their applications. *Advances in Colloid and Interface Science* **2014**, *214*, 17 –37.

(28) Szczurek, A.; Barcikowski, M.; Leluk, K.; Babiarczuk, B.; Kaleta, J.; Krzak, J. Improvement of Interaction in a Composite Structure by Using a Sol-Gel Functional Coating on Carbon Fibers. *Materials* **2017**, *10*, DOI: `10.3390/ma10090990`.

(29) Latella, B. A.; Swain, M. V.; Ignat, M. In *Nanoindentation in Materials Science*, Nemecek, J., Ed.; IntechOpen: Rijeka, 2012; Chapter 6.

(30) Metroke, T. L.; Kachurina, O.; Knobbe, E. T. Spectroscopic and corrosion resistance characterization of GLYMO–TEOS Ormosil coatings for aluminum alloy corrosion inhibition. *Progress in Organic Coatings* **2002**, *44*, 295 –305.

(31) Dalmoro, V.; dos Santos, J.; Alemán, C.; Azambuja, D. An assessment of the corrosion protection of AA2024-T3 treated with vinyltrimethoxysilane/(3-glycidyloxypropyl)trimethoxysilane. *Corrosion Science* **2015**, *92*, 200 –208.

(32) Juan-Díaz, M.; Martínez-Ibáñez, M.; Hernández-Escolano, M.; Cabedo, L.; Izquierdo, R.; Suay, J.; Gurruchaga, M.; Goñi, I. Study of the degradation of hybrid sol–gel coatings in aqueous medium. *Progress in Organic Coatings* **2014**, *77*, 1799 –1806.

(33) Crundwell, F. K. On the Mechanism of the Dissolution of Quartz and Silica in Aqueous Solutions. *ACS Omega* **2017**, *2*, 1116–1127.

(34) Morgan, M. R. Characterizing the Effects of Capillary Flow During Liquid Composite Molding., MA thesis.

(35) Martinez-Ibañez, M.; Aldalur, I.; Romero-Gavilán, F.; Suay, J.; Goñi, I.; Gurruchaga, M. Design of nanostructured siloxane-gelatin coatings: Immobilization strategies and dissolution properties. *Journal of Non-Crystalline Solids* **2018**, *481*, 368 –374.

(36) EL-Dessouky, H. M.; Lawrence, C. A. Ultra-lightweight carbon fibre/thermoplastic composite material using spread tow technology. *Composites Part B: Engineering* **2013**, *50*, 91 –97.

(37) Koncherry, V.; Potluri, P.; Fernando, A. Multifunctional Carbon Fibre Tapes for Automotive Composites. *Applied Composite Materials* **2017**, *24*, 477–493.

(38) Metroke, T. L.; Gandhi, J. S.; Apblett, A. Corrosion resistance properties of Ormosil coatings on 2024-T3 aluminum alloy. *Progress in Organic Coatings* **2004**, *50*, 231 –246.

(39) Zīle, E.; Zīle, O. Effect of the fiber geometry on the pullout response of mechanically deformed steel fibers. *Cement and Concrete Research* **2013**, *44*, 18 –24.